Transport and optical properties of a-GaP prepared at different substrate temperatures

1994 J. Phys.: Condens. Matter 6 779

(http://iopscience.iop.org/0953-8984/6/3/018)

J. Phys.: Condens. Matter 6 (1994) 779–790. Printed in the UK

Transport and optical properties of a-GaP prepared at different substrate temperatures

N Elgun and E A Davis

Department of Physics and Astronomy, University of Leicester, Leicester LE1 7RH, UK

Received 27 July 1993, in final form 19 October 1993

Abstract. The electronic properties of a series of nearly stoichiometric sputtered a-GaP films have been investigated as a function of increasing deposition and annealing temperatures up to 270 °C. The optical absorption coefficient ($10\ cm^{-1} < \alpha < 10^5\ cm^{-1}$) as a function of photon energy, deduced both from transmission (T) and reflection (R) measurements and from photothermal deflection spectroscopy (PDS), shows a very large shift of the edge towards lower energies relative to that of c-GaP. The electrical conductivity data have an activation energy that varies continuously with temperature. The results are related to the atomic structure of films which was reported earlier by Elgun, Gurman and Davis and also to the microstructure which is shown to contain voids. In addition, a density-of-states picture based on theoretical calculations by O'Reilly and Robertson is used for interpretation of the results.

1. Introduction

Crystalline GaP is widely used in technological applications such as light-emitting diodes and high-temperature transistors. It is also one of the basic materials for alloy semiconductor lasers and superlattice devices. Similarly, their amorphous counterparts have become of technological interest recently, and they have already been used in the fabrication of electroluminescent diodes where green light is obtained [1]. Furthermore, junction diodes composed of p-type a-GaP:H films doped with Zn on n-type c-GaP substrates show good rectification properties [2]. Yet, from the fundamental research point of view, chemical disorder and other defects in the a-GaP structure, which influence the valence- and conduction-band densities of states and therefore the electronic properties, have not been completely resolved.

Identification and quantification of chemical disorder as exemplified by wrong bonds have attracted considerable attention since such defects are considered to be probable for topological reasons. An early model of a continuous random network with odd-membered rings, namely the Polk model, necessarily requires wrong bonds in the a-GaP network. Later on, Dixmier *et al* [3] showed that the Connell–Temkin model, which is again a continuous random network but with even-membered rings only, was more appropriate. This suggests that a-GaP is chemically ordered. However, it seems that the existence of chemical disorder depends strongly on the sample preparation of technique. For flash-evaporated samples, a proportion of wrong bonds as high as 25% has been reported [4]. In contrast, Elgun *et al* [5] found no (or very few, below the detection limits of extended x-ray absorption fine structure (EXAFS) and infrared (IR) spectroscopy) wrong bonds for RF-sputtered a-GaP samples.

Another probable defect is the dangling bond. There have been only a few studies to identify and quantify these in a-GaP. They can exist in isolation as well as at the inner

0953-8984/94/030779+12$07.50

surfaces of voids in the network, which may occur in order to relieve strain, and have been identified by electron spin resonance (ESR) [6]. According to O'Reilly and Robertson [7], about 2% dangling bonds for each constituent atom may be expected.

Reports on a-GaP prepared by a variety of vapour-deposition techniques can be found in the literature. Evaporated a-GaP films have been studied most extensively [8–11], and their structure and electronic properties have been investigated in a systematic way. Glow-discharge samples have also been prepared [12]. For RF-sputtered a-GaP, there have been some preliminary results [13–15] on electronic properties in a limited range. Recently, we have reported [5] a detailed structural study of RF-sputtered, nearly stoichiometric, a-GaP as a function of deposition temperature. In this paper, we present the optical and electrical properties of these films, and discuss the results in relation to the structure in order to obtain more information about the effect of the defects on the density of states in the valence and conduction bands.

2. Experimental procedures

2.1. Sample preparation

The samples used in this study were prepared by RF sputtering, which was carried out in an argon atmosphere at a pressure of 3–4 mTorr. The base pressure of the system was 2×10^{-7} mTorr. An RF power input of 250 W was applied to the 4″ stoichiometric polycrystalline GaP target, which was positioned 5 cm away from the substrates. The temperature of the substrates during deposition was varied between room temperature and 200 °C, and the corresponding deposition rates were in the range 30–40 Å min^{-1}. Annealing at higher temperatures was carried out in a vacuum of 10^{-5} mTorr for 2 h.

Films for optical and electrical measurements were deposited on fused silica and Corning 7059 glass substrates respectively, and had thicknesses of 1–1.2 μm. Electron-microscope samples (~100 Å thick) were deposited on mica, then floated off in water and transferred to Cu grids. A 260 μm thick undoped c-GaP sample, supplied by the Philips Research Laboratories, was used for comparative optical measurements.

The thicknesses of the films were determined both by an optical technique, in which the interference fringes in reflection were used, and by a mechanical method using a Talysurf. The results agreed to within 5%.

2.2. Methods of measurement

The DC conductivity measurements were performed using the two-probe technique for which gold or aluminium electrodes were evaporated onto the film surface in a co-planar configuration. Leads were made to the electrodes with fine gold wire attached by a silver-loaded electrically conducting paste. The current–voltage curves were found to be linear. The conductivity measurements were carried out using a stabilized power supply and a Keithley 616 electrometer in the temperature range 1500–520 K in a cryostat filled with an overpressure (~2–3 psi) of helium after being evacuated to 10^{-6} mTorr.

The optical transmission T and reflection R measurements were made at room temperature in the ultraviolet (UV)/visible/near-IR region with a Perkin–Elmer 330 double-beam spectrophotometer. In all the samples investigated, T and R displayed interference fringes due to multiple reflections within the film and substrate, which became more pronounced at lower energies. The extrema of the fringes in the reflection were used to calculate the refractive index n and thickness t of the films by the method proposed in

[16]. The absorption coefficients in the range of 10^3–10^5 cm^{-1} were determined from the approximate formula

$$T = (1 - R)\exp(-\alpha t)$$

where the measured transmission T and reflection R values were taken from the region in which fringing is slight or absent, in order to minimize the error in α.

Low absorption coefficients down to 10 cm^{-1} were obtained using photothermal deflection spectroscopy (PDS), a method introduced by Jackson *et al* [17]. The PDS measurements were carried out in the transverse mode with a 100 W tungsten–halogen lamp as the pump beam, which was modulated at a frequency of 7 Hz, and a 0.5 mW helium–neon laser as the probe beam. The deflection medium was CCl_4, and both Si and PbS detectors were used for normalization of the pump beam intensity. The PDS spectra were calibrated by adjusting to the absorption coefficient values deduced from T and R measurements in the 10^4 cm^{-1} range. The combination of T, R and PDS data gave an optical absorption spectrum extending over three to four orders of magnitude in α.

3. Results

3.1. Microstructure

The compositions of the films were determined by a DS 130 scanning electron microscope to which an energy-dispersive x-ray analyser (EDAX) was attached and also by EXAFS measurements. The latter method is described in detail in [5]. All samples were found to be stoichiometric to within a few percent. EDAX was also used to probe the compositional fluctuations of the films. For this purpose, line profiles shown in figure 1 have been taken across the films for both Ga and P atoms. It was found that for some films, while the Ga content is stable, the P content shows small fluctuations, possibly due to plasma instabilities during the deposition process.

The microstructure of the films was also investigated using a Joel Jem 100Cx transmission electron microscope. The electron diffraction patterns confirmed that the films are amorphous. Bright-field electron micrographs in real space have revealed the presence of voids. Figure 2(a) shows a micrograph for an a-GaP film prepared at 200 °C, in which dark and light regions correspond to the film and voids, respectively. The sizes of the dark regions were measured and found to be between 280 and 560 Å. In order to demonstrate that these regions are not small crystals oriented in different directions, the diffraction pattern of the same film is shown in figure 2(b).

It seems that the deposition temperature T_s should be higher than 200 °C to obtain void-free a-GaP films. As the deposition temperature was lowered, it was observed that the dark regions became smaller, implying an increase in the void concentration. It was also inferred that the void sizes decrease with decreasing T_s. For films deposited at room temperature, the voids could not be seen by transmission electron microscopy with a resolution of order 100 Å. Small-angle scattering experiments on this sample have revealed voids 60 Å in diameter on average. The small-angle scattering experiments have also revealed no additional peak at high q in the $I(q)$ versus q plots, which would be taken as indicative of phase separation [18].

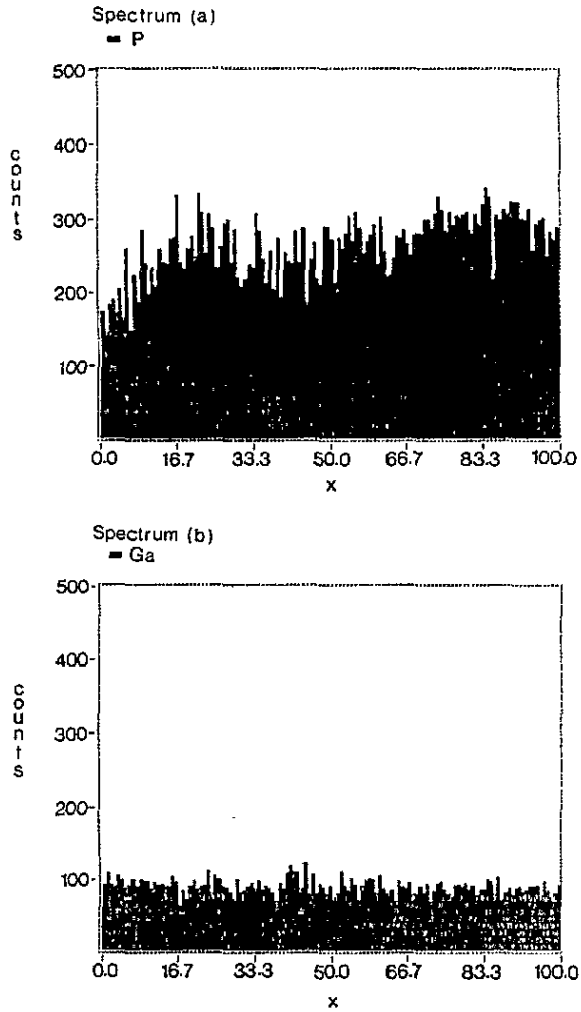

Figure 1. Line profiles of (a) P, (b) Ga taken by EDAX. x = 100 is approximately 1 mm.

3.2. Optical properties

The dispersion of the refractive index n for a-GaP films deposited at different temperatures is presented in figure 3. The refractive index of c-GaP taken from [19] and [20] is also included for comparison. It is seen that n increases with photon energy as the fundamental absorption edge is approached, and the values for the amorphous films at a given photon energy decrease towards the crystalline value as T_s is increased.

Figure 4 shows the optical absorption coefficient α deduced from both R–T and PDS measurements as a function of photon energy for amorphous films deposited at different temperatures and a crystalline wafer. The data reported in [8] for bulk c-GaP have also been added to the figure (broken curve) to display the direct and indirect optical gaps, which occur at 2.78 eV and 2.26 eV, respectively. The tailing of the absorption below 1 cm^{-1} indicates a wide energy range for defects or impurity states in the optical gap of the crystal. As for the absorption-edge spectrum of the amorphous film, the striking feature is that it shows a very large shift (~1.6 eV) towards lower photon energies compared with that of

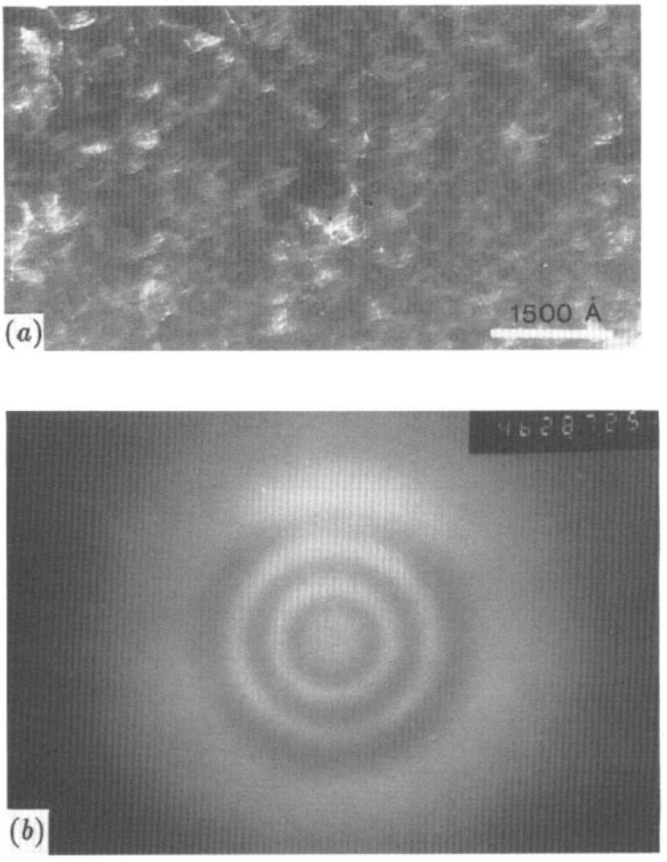

Figure 2. (*a*) Bright-field electron micrograph of an a-GaP (T_s = 200 °C) film. Dark and light regions correspond to film and voids, respectively. (*b*) Electron diffraction pattern of the same film.

the crystal. In fact, this is the largest shift found amongst amorphous group-IV and III–V semiconductors. This is why previous studies [14, 21] have invoked the existence of wrong bonds in the network. Also, the edge itself is very broad and becomes even broader with increasing deposition temperature as opposed to the case for a-Si and a-Ge.

The absorption-edge spectra of the amorphous samples are seen to consist of two regions, namely power-law and Urbach regions. The power-law region, i.e. the non-exponential part of the absorption coefficient data ($\alpha \geqslant 10^4$ cm^{-1}), was used to determine the optical gaps. The data were fitted to the relation given below for the Tauc gap E_T:

$$(\alpha\hbar\omega)^{1/2} = B(\hbar\omega - E_T)$$

where B is a constant. Also, the photon energy values corresponding to $\alpha = 10^4$ cm^{-1} have been used for the E_{04} gap. Figure 5 shows the variation of both the optical gaps, E_T and E_{04}, with the deposition temperature. For samples prepared at room temperature, the Tauc gap is 1.0 eV and increases first gradually, then rapidly at about 150–170 °C, reaching 1.36 eV when T_s is 200 °C. E_{04} follows the same trend. These optical gap values seem to be in good agreement with the value of 1.17 eV given for the magnetron sputtered samples

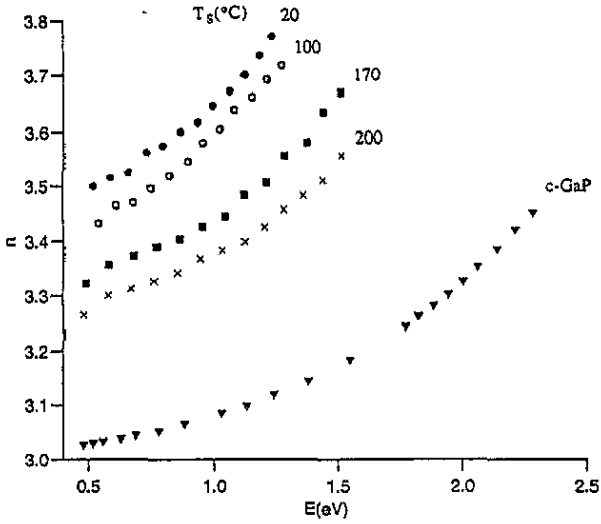

Figure 3. Dispersion of the refractive index for a-GaP films deposited at different temperatures. Data for c-GaP from [19] and [20] is included for comparison.

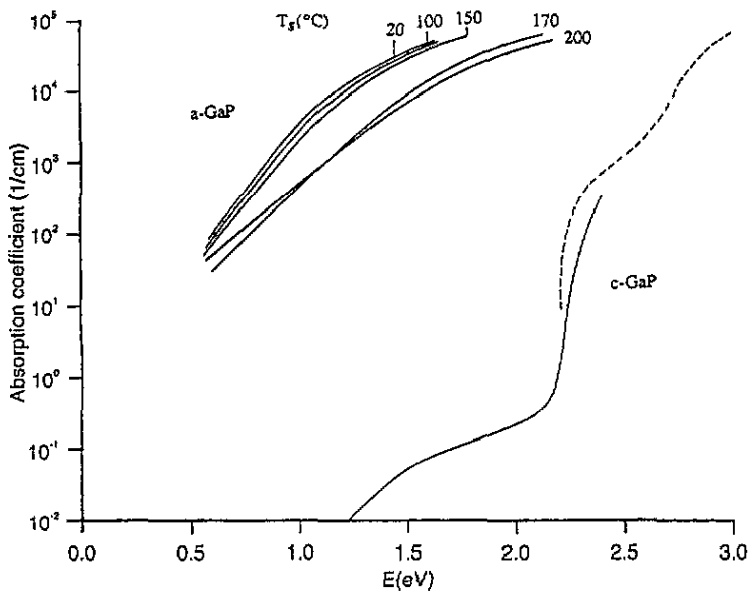

Figure 4. Absorption coefficient spectra deduced from T, R and PDS measurements for a-GaP films prepared at different deposition temperatures and for a c-GaP wafer. The broken line refers to the data for bulk c-GaP reported in [8].

of Matsumoto *et al* [15] but bigger than the 0.42 eV reported in the early work of Connell *et al* [14]. Gheorghiu and Theye [10] have found 1.2–1.4 eV for as-deposited and 1.5–1.7 eV for annealed flash-evaporated samples.

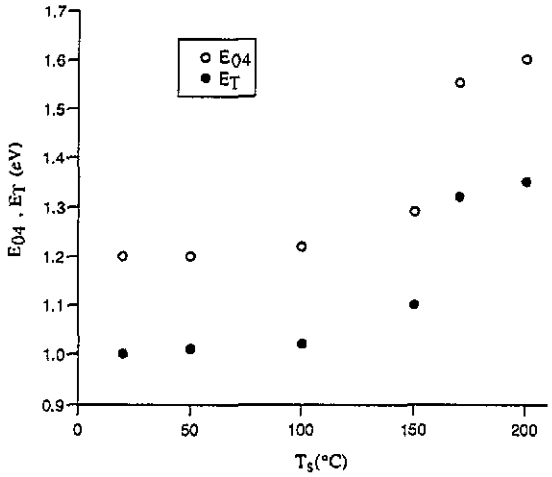

Figure 5. Variation of the optical gaps E_{04} and E_T with deposition temperature.

The Urbach region, i.e. the exponential part of the absorption coefficient data ($\alpha \leqslant 10^3$ cm^{-1}), was fitted to the relation of the form

$$\alpha = \alpha_0 \exp(\hbar\omega/E_U)$$

in order to determine the Urbach slope E_U. The values obtained for E_U are 112, 118, 125, 158 and 187 meV for T_s = 20, 100, 150, 170 and 200 °C, respectively. To our knowledge, there are no data available in the literature for comparison.

3.3. Electrical conductivity

Figure 6 presents the variation of conductivity as a function of inverse temperature for a-GaP films prepared at different deposition temperatures T_s and with annealing temperatures T_a. For all the films, the conductivity cannot be described by the simple activated form of $\sigma(T) = \sigma_0 \exp(-E_a/kT)$ with a single activation energy E_a, but instead exhibits a curvature over the entire temperature range studied, resulting in a continuously varying activation energy. E_a increases from 0.23 eV to 0.36 eV with rising T for samples deposited at 20 °C and from 0.11 eV to 0.48 eV after annealing at 270 °C. Values for the pre-exponential factor σ_0, which normally provides information on the conduction mechanism involved, were obtained from extrapolations of the tangents to the curves at the high-temperature ends; they lie between 2 and 50 Ω^{-1} cm^{-1} for the T_s, T_a range of 20–270 °C. The low values of σ_0, in addition to the curvature of the conductivity plots, rule out the possibility that the conduction is via extended states in either the valence or conduction bands.

A relation of the form σ = constant $\exp[-(T_0/T)^{1/4}]$, which expresses variable-range hopping conduction at the Fermi level, has also been tested. The plots of ln σ versus $T^{-1/4}$ were linear up to very high temperatures, with $T_0 = 3 \times 10^9$ for as-deposited samples and slightly higher for samples deposited or annealed at a higher temperature. However, the density of states calculated from the values of T_0 (assuming a localization length of 10 Å) were unreasonably high, which led us to believe that variable-hopping at the Fermi level is not the mechanism for conduction either.

A possible mechanism for these films seems to be transport taking place in a band tail, in which the conduction path moves down in the tail states at T is lowered, producing a

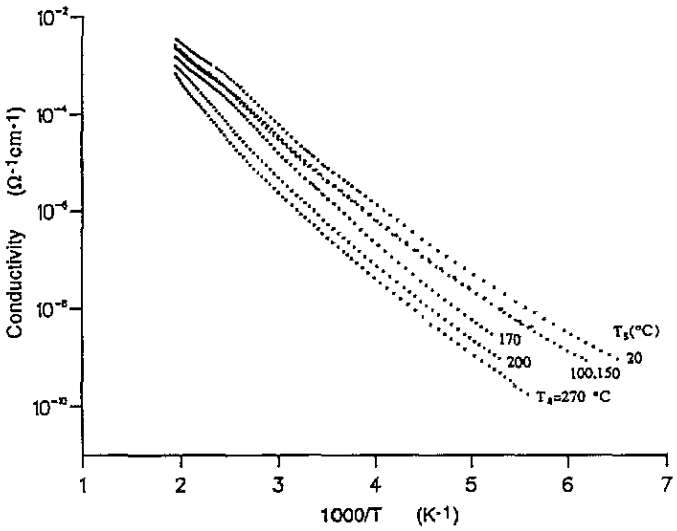

Figure 6. Conductivity as a function of inverse temperature for a-GaP films with different temperatures T_s and T_a of deposition and annealing, respectively.

gradually decreasing activation energy. Such a mechanism is also consistent with the low values of σ_0.

In figure 6, a kink can be seen at the high-temperature end of some of the curves. This kink, which was observed only during the heating cycle, was found to occur at 115 °C for samples deposited at room temperature and was shifted towards higher temperatures for samples prepared at high deposition temperatures and in annealed samples. It was attributed to *in situ* annealing affects, which are indicative of a loose structure possibly stemming from the presence of voids in the network. Figure 6 also shows a reduction in the conductivity values for samples prepared at high T_s and T_a.

It appears that our conductivity data are quite different from the only conductivity report [15] in the literature on sputtered a-GaP, although the optical-gap values are in good agreement as we mentioned earlier. The measurements of Matsumoto and Kumabe [15] reveal a kink at a critical temperature T_c of 150 °C, above and below which activated conduction occur. They have assigned the activation energy above T_c to intrinsic activation, and that below T_c (0.42 eV) to the energy between extended and gap states. For flash-evaporated films prepared at room temperature, an exponential variation of conductivity has been observed [22], whereas annealed samples showed an activated behaviour with a single activation energy of 0.4–0.5 eV above room temperature, indicating transport in extended states beyond the mobility edge [10]. However, since the pre-exponential factor was not compatible with extended-state conduction and E_a was much smaller than half the optical gap E_T, the same results were also interpreted as activated hopping in band tails [21]. At low temperatures, the conductivity data were found to follow the law $\sigma = \sigma_0 \exp(T_0/T)^n$ with $n = \frac{1}{4}$ and T_0 of the order of 10^9 K for as-deposited samples, and $n = \frac{1}{2}$ for annealed samples [21].

4. Discussion

Recently, O'Reilly and Robertson [7] have reported a comprehensive theoretical study on amorphous III–V semiconductors. Using the tight-binding recursion method, they calculated local densities of states of bulk and defect sites. The calculations for the bulk sites show that both the valence- and conduction-band edges should not be affected by any variations in bond angle, and hence theoretically little change in the band gap is expected from this source. However, since experimentally the optical gaps are found to be smaller than those in the corresponding crystals, they invoke the presence of significant numbers of defect states. Two types of defect, namely dangling bonds and wrong bonds, have been studied. It was found for a-GaP that the unrelaxed singly occupied P and Ga dangling bonds give rise to states at or close to the valence- and conduction-band edges, respectively. These bonds can become doubly occupied, whereupon they relax by altering their environment from fourfold to threefold coordination, accompanied by a change of the tetrahedral bond angle of 109° to the preferred angles of 97° and 120° for P and Ga dangling bonds, respectively. In this case, the corresponding states move into the valence and conduction bands. The singly occupied dangling bonds can also interact with one another either forming weak bonds or creating dangling-bond–defect complexes, which are likely to occur at the inner surfaces of voids. The calculations have shown that a complex of two adjacent P dangling bonds produces states nearer to midgap. Furthermore, they have revealed that isolated wrong bonds, i.e. Ga–Ga and P–P, give rise to states near the valence- and conduction-band edges, respectively, whereas clusters of wrong bonds produce states near midgap. Figure 7 illustrates a schematic diagram of the density of states of c-GaP close to the band edges together with the calculated positions of the states that arise from different types of defect possible in an a-GaP network [7]. For sputtered a-GaP, our EXAFS and IR data [5] have shown that there are no or very few wrong bonds in the network. This result is supported by the electron spin resonance (ESR) study of Hoheisel *et al* [6] who assigned resonance signals to dangling bonds rather than wrong bonds. Therefore, the states due to isolated wrong bonds should be insignificant in the density-of-states picture. On the contrary, since our samples were found to contain voids, we expect a significant number of dangling bonds. Hoheisel *et al* [6], however, have found the spin density of P and Ga dangling bonds to be of the order of 10^{18} and 10^{17} cm^{-3}, respectively, which suggests that most of the dangling bonds are either relaxed or they have linked to one another in such a way that the remaining number of unpaired electrons is very few.

One can note in figure 7 that the states arising from both the unrelaxed and relaxed dangling bonds have accumulated into the band edges, producing a high density of tail states, which inevitably results in a reduction in the band gap and hence a shift of the absorption edge towards lower energies. However, it is clear that these states alone are insufficient to account for the observed 1.6 eV shift of the edge. In order to explain such a large shift, the states due to defect complexes (e.g. $P(db)_c$, $Ga(db)_c$), which are located nearer to midgap, should be taken into account. Since these defect complexes cause a small absorption, they can be related to the low-energy part of the absorption-edge spectra, whereas the isolated dangling bonds are associated with the high-energy part of the edge. It is probably easier to eliminate the isolated defects rather than the defect complexes. Hence, as the deposition or annealing temperature is increased, the isolated defects are for the most part annealed out, resulting in a larger shift in the high-energy part of the absorption edge [23] compared to the shift in the low-energy part of the edge back towards the crystalline position. Therefore, the Urbach edge becomes broader with increasing T_s. If T_s is increased above 400 °C, these defect complexes are eventually annealed out and the Urbach edge becomes sharper as demonstrated by Davey and Pankey [8] on evaporated films.

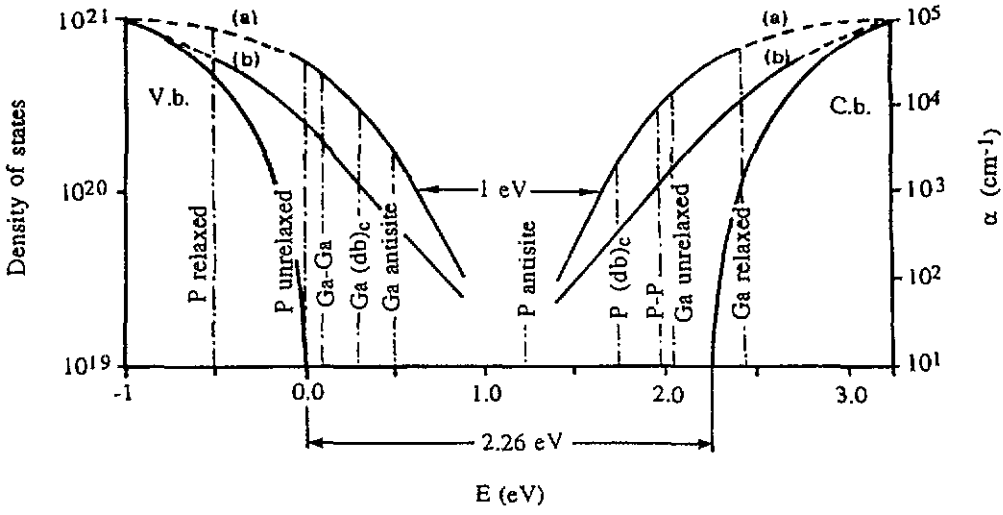

Figure 7. A schematic diagram of the density of states of c-GaP close to the band edges and closure of the band gap arising from the different types of defect state for a-GaP (T_s = 20 °C) (curves a) a-GaP (T_s = 200 °C) (curves b). $Ga(db)_c$ defects are positioned by analogy with $P(db)_c$.

As seen in figure 7, there is no particular gap state with a high density in the pseudo-gap and the residual density of states is very low. This can explain the absence of subgap absorption in the absorption edge of a-GaP, as compared to the case for a-Si:H. It is also consistent with the absence of a variable-range hopping mechanism in the conductivity data. The conductivity, instead, is more likely to be dominated by a transport mechanism taking place in such wide tails. With annealing and increasing deposition temperature, since there will be removal or relaxation of the defects and hence a lowering of the density of states, as seen in figure 7, the conductivity is reduced relative to the room-temperature-deposited sample but hopping in the tail states still occurs. The activation energies found, however, cannot be used to correlate the conductivity data to the optical data in order to obtain information about the position of the Fermi level.

The optical properties of a semiconductor can be correlated to its structural properties using the refractive-index data. This is done by relating the static refractive index $n(0)$ (n at zero energy) to the plasma frequency ω_p of the valence electrons by the following expression [25]:

$$n(0)^2 = 1 + \tfrac{2}{3}(\hbar\omega_p/E_g)^2$$

where E_g is the Penn gap, which represents an average separation between valence and conduction bands and is therefore a measure of the bond strength. The plasmon energy of a-GaP is found to be smaller than that of the crystal [26], and hence the increase in $n(0)$ for a-GaP, as shown in figure 3, indicates a reduction in its Penn gap. The figure also shows a decrease in $n(0)$ for amorphous samples with increasing deposition temperature T_s, which could arise from either a decrease of $\hbar\omega_p$ or an increase of E_g or both. In principle, changes in the Penn gap can result from variations in bond length ($E_g \propto r^{-2.5}$), coordination number ($E_g \propto N^2$) and bond-angle distribution [24]. The first two effects are ruled out by our EXAFS

data on sputtered a-GaP [5], which revealed, within experimental uncertainties, no changes in bond length and coordination number. However, a considerable reduction in the spread of the bond angle was observed as T_s increased from 20 to 200 °C. From IR spectroscopy, it was found that this reduction in the spread of the bond angle is associated with a 15% increase in the strength of the Ga–P bond [5]. From the above equation, this should reduce $n(0)$ by about 12%. However, experimentally a decrease of only 5% is found when T_s is increased from 20 to 200 °C. This suggests that the rise in E_g is partially compensated by an increase in $\hbar\omega_p$. An increase in $\hbar\omega_p$ is expected when densification, arising both from a reduction in void concentration and from local atomic rearrangements, occurs with increasing T_s.

The above arguments apply only if the voids are small enough to be accessible to the electrons. If the voids are large, effective-medium theory predicts an overall increase in $n(0)$ when their concentration is reduced by annealing [24,27]. Although we cannot rule out a contribution of this nature, the experimental result of a decrease in $n(0)$ on annealing shows that the effect cannot be dominant. Small-angle x-ray scattering experiments on the samples after annealing would be informative.

5. Conclusions

In this paper, we have presented the electronic properties of nearly stoichiometric sputtered a-GaP films prepared at different deposition temperatures and after annealing. It was shown that the principal optical results and also the conductivity of the samples can be explained by a density-of-states picture taking into account the defect states, mainly dangling bonds and their complexes, located at positions calculated by O'Reilly and Robertson [7].

Acknowledgments

The authors gratefully acknowledge G L C McTurk and C D'Lacey for the SEM and TEM experiments, Dr S J Gurman and B T Williams for the small-angle scattering experiments, and Dr S H Baker for useful discussions. N Elgun wishes to thank Ege University in Turkey for the award of a studentship.

References

[1] Kubota H and Onuki M 1989 *J. Non-Cryst. Solids* **115** 39
[2] Fujiyoshi T, Onuki M, Homnyo K, Kubota H and Matsumoto T 1991 *J. Non-Cryst. Solids* **137&138** 935
[3] Dixmier J, Gheorghiu A and Theye M L 1984 *J. Phys. C: Solid State Phys.* **17** 2271
[4] Udron D, Flank A M, Gheorghiu A, Lagarde P and Theye M L 1989 *Physica* B **158** 625
[5] Elgun N, Gurman S J and Davis E A J 1992 *J. Phys.: Condens. Matter* **4** 7759
[6] Hoheisel B, Stuke J, Stutzmann M and Beyer W 1985 *Proc. 17th Int. Conf. on the Physics of Semiconductors (New York, 1985)* ed J D Chadi and W A Harrison (Berlin: Springer) p 877
[7] O'Reilly E P and Robertson J 1986 *Phys. Rev.* B **34** 8684
[8] Davey J E and Pankey T J 1969 *Appl. Phys.* **40** 212
[9] Stuke J and Zimmerer G 1972 *Phys. Status Solidi* b **49** 513
[10] Gheorghiu A and Theye M L 1980 *J. Non-Cryst. Solids* **35&36** 397
[11] Onuki M, Tsubusaki K and Kubota H J 1987 *J. Non-Cryst. Solids* **97&98** 1347
[12] Knights J C and Lujan R A 1978 *J. Appl. Phys.* **49** 1291
[13] Sosniak J 1970 *J. Vac. Sci. Technol.* **7** 110
[14] Connell G A N and Paul W 1972 *J. Non-Cryst. Solids* **8–10** 215

[15] Matsumoto N and Kumabe K 1979 *Japan. J. Appl. Phys.* **18** 1011
[16] Cisneros J I, Rego G B, Tomyiama M, Bilac S, Goncalves J M, Rodriguez A E and Arguello Z P 1983 *Thin Solid Films* **100** 155
[17] Jackson W B, Amer N M, Boccara A C and Fournier D 1981 *Appl. Opt.* **20** 1333
[18] Rice M, Bienenstock A and Wakatsuki S 1991 *Stanford Synchrotron Radiation Laboratory Annual Report*
[19] Bond W L 1965 *J. Appl. Phys.* **36** 1674
[20] Nelson D F and Turner E H J 1969 *J. Appl. Phys.* **39** 3337
[21] Gheorghiu A and Theye M L 1981 *Phil. Mag.* **4** 285
[22] Beyer W 1974 *PhD Thesis* University of Marburg
[23] The absorption edge shifts towards higher energies slowly below T_s = 150 °C, but between 150 and 170 °C a rapid shift occurs. The dependence of α and other film properties, such as refractive index and spread in bond angle, on T_s in this way suggests that film growth during deposition is controlled by an activated process in which local surface reorganizations occur above a critical deposition temperature [24].
[24] Paul W, Connell G A N and Temkin R J 1973 *Adv. Phys.* **22** 529
[25] Cardona M 1971 *'Enrico Fermi' School of Physics (Varenna, 1971)*
[26] Schevchik N J, Tejeda J and Cardona M 1974 *Phys. Rev.* B **9** 2627
[27] Gurman S J 1992 *J. Non-Cryst. Solids* **143** 207